

# Identification and Analysis of Hydrodynamic and Transport Characteristics of Cannonsville Reservoir

E. M. Owens

*Department of Civil and Environmental Engineering  
Syracuse University, Syracuse, NY 13244*

## ABSTRACT

Owens, E. M. Identification and analysis of hydrodynamic and transport characteristics of Cannonsville Reservoir. *Lake and Reservoir Management*. 14(2-3):162-171.

A monitoring program consisting of regular observations of temperature and conductivity in the tributaries to and water column of Cannonsville Reservoir from April through November of 1995 is described. The results are analyzed in order to identify and quantify transport processes that affect the distribution of heat and mass constituents. The low temperature of the major reservoir tributary relative to reservoir surface waters in late summer and fall is observed to cause a plunging inflow or negatively-buoyant density current in the reservoir, although evidence is provided that the plunging inflow is not the cause of the observed metalimnetic oxygen minima. A seasonal increase in the specific conductivity of the major tributary in summer creates a longitudinal gradient in conductivity in the epilimnion of the reservoir. A simple analytical model is used to estimate the longitudinal dispersion coefficient in the epilimnion over the summer based on this conductivity gradient. High-frequency observations of temperature using thermistor chains deployed late in the summer stratification period indicate the presence of internal waves in the stratified layers of the reservoir. Current measurements indicate the occurrence of episodes of current speed of a magnitude sufficient to cause sediment resuspension. The application of hydrothermal models to the reservoir to support water quality management is discussed.

**Key Words:** inflow mixing, vertical transport, hydrothermal model.

The spatial and temporal distribution of temperature and dissolved or suspended mass constituents in a reservoir is regulated by both physical and biochemical processes. The biochemical processes describe the cycling of materials through various forms in the water column and perhaps the underlying sediments (Chapra 1997). The physical processes describe the transport of heat and mass constituents through the water column and at the sediment-water interface. Under the turbulent flow conditions which exist in reservoirs, the quantities describing the movement (velocity) and mixing (diffusion or dispersion coefficients) are the same for heat and all mass constituents (Fischer et al. 1979), with the exception that settling velocities and resuspension characteristics of particulate materials may vary.

The basic transport characteristic of water velocity may be measured with current meters or drogues. However, a more useful measure of large-scale transport is the movement of tracers. Away from the influence of heat transfer at the water surface, temperature may be used as such a tracer, particularly in the study of vertical mixing under the conditions of thermal stratification (Fischer et al. 1979). High-frequency temperature observations can also indicate the presence of motion

associated with internal waves (Lemmin 1987). Alternatively, dissolved solids or salinity may be used as a tracer if spatial gradients in these constituents are present. Of course, both temperature and dissolved solids affect water density, and density differences between reservoir and tributary waters may result in buoyancy-driven water motion and transport (Fischer et al. 1979, Ford and Johnson 1983). A monitoring program which includes selected physical measurements of temperature, dissolved solids, and water motion allows important transport processes to be identified and quantified.

Here I describe the occurrence and magnitude of selected transport characteristics of Cannonsville Reservoir that were identified from a monitoring program conducted from April through November of 1995. The program included observations of tributary and reservoir temperature and conductivity, outflow temperatures, and currents. The observations described here were a part of a larger program that was designed to support the development of hydrothermal and eutrophication models for the reservoir. The analysis of the monitoring data provided here serves both to describe the spatial and temporal dynamics of the observations, and to identify potentially important

underlying physical processes that should be included or analyzed in hydrothermal models of the reservoir (Owens 1998b, Gelda et al. 1998). These models are designed to provide a quantitative linkage between hydrologic, meteorologic, and reservoir operations conditions, and the resulting dynamics of water temperature and transport processes in the reservoir. These models may then be used in the analysis of water quantity and quality management alternatives.

Cannonsville Reservoir is a water supply and flow augmentation impoundment owned and operated by New York City Department of Environmental Protection (NYCDEP). At full capacity the reservoir has mean and maximum depths of 19 and 50 m, respectively. Two major tributaries, the West Branch of the Delaware River (WBDR) and Trout Creek (TC) enter the two "arms" of the long, narrow basin (Fig. 1). Reservoir outflow occurs in three forms: over a spillway located adjacent to the dam (spill), through release ports located at the base of the dam (release), or through one of three drinking water intake structures (Fig. 1) that are located at different elevations (withdrawal).

## Methods

Temperature and conductivity were measured weekly at six sites in the reservoir (Fig. 1) from April through November of 1995, a total of 37 dates. Measurements were made at 0.5 m depth intervals. In addition, temperature and conductivity sensors were deployed at a depth of 0.5 m at sites 1 and 4 (Fig. 1), recording at an hourly frequency, from 11 April until 9 October. The temperature and conductivity of WBDR and TC inflows were monitored with deployed temperature and conductivity sensors recording at an hourly frequency on 101 and 129 days during the April-October period for WBDR and TC, respectively. In addition, single biweekly daytime temperature and conductivity measurements were made at the tributary mouths. All

conductivities were corrected to 25 °C. In order to quantify the effect of temperature and conductivity on water density, an equation of state that relates density to temperature and total dissolved solids (TDS) concentration was used. TDS is computed from temperature-corrected conductivity using the empirical relationship  $TDS = 0.64C$  where  $C$  is the conductivity ( $\mu\text{mhos} \cdot \text{cm}^{-1}$ ) corrected to 25 °C.

Reservoir water surface elevation and the rate of each form of reservoir outflow are recorded as daily averages by NYCDEP. The temperature of water released from the base of the dam is measured in the river channel 2.4 km downstream of the dam. The temperature of the drinking water withdrawal is measured from sampling taps that lead from each of the three intake structures. A meteorological station was installed at the Cannonsville Dam throughout 1995. Among other quantities, wind speed and direction were measured at an hourly interval.

Thermistor strings (Aanderaa Model 2862) and associated data loggers (Aanderaa Model TR7) were installed at sites 1 and 4 (Fig. 1) for the period 13 September to 10 October. At site 1, eight thermistors located over a depth range from 1.3 to 18.8 m, at a uniform interval of 2.5 m were deployed. At site 4, 11 thermistors over depth from 1.3 to 18.8 m at a uniform interval of 1.25 m were used. The thermistor chains were suspended from surface buoys, so that the position of the thermistors relative to the changing water surface elevation remained fixed. At both sites, temperatures were recorded every 10 minutes. Current meters (Endeco Model 174) were also deployed for the same period and at the same sites as the thermistor strings. The current meters were moored from bottom anchors and remained at a fixed elevation, but variable depth below the changing reservoir water surface elevation, over the period of deployment. At site 1, the current meter was located at elevation 323.0 m, or 10 m above the bottom, while at site 4 the meter was located at elevation 323.6 m, or 2.5 m above the bottom at that location.

## Results

Significant reservoir drawdown occurred in 1995 (Fig. 2) as a result of low tributary inflow and sustained reservoir withdrawal and release through the spring and summer (Owens et al. 1998). The large drawdown resulted in a relatively early fall turnover in the first week in October (Owens 1998a). Thermal stratification was observed in the reservoir (Fig. 3), and vertical variations in conductivity were also detected. However, the contribution of conductivity to vertical variation in water density was very small, so that for practical

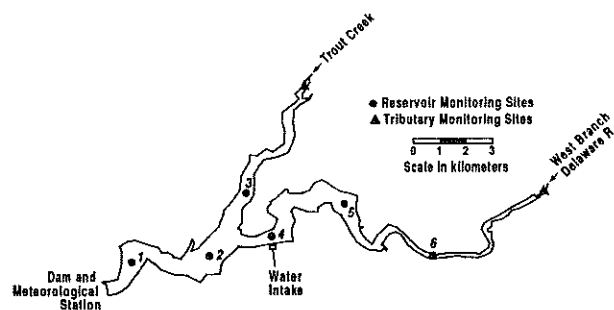


Figure 1.—Map of Cannonsville Reservoir, showing location of dam and drinking water intakes, major tributaries, reservoir monitoring sites, and tributary monitoring sites.

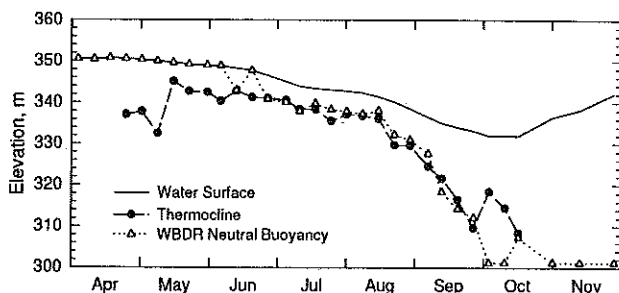


Figure 2.—Selected reservoir characteristics for 1995: (a) water surface elevation; (b) thermocline elevation; and (c) neutral buoyancy elevation of WBDR inflow.

purposes water column variations in density can be determined from temperature only. The average and maximum density differences over the water column at site 1 associated with top-bottom differences in *TDS* were 0.0036 and 0.028  $\text{kg}\cdot\text{m}^{-3}$ , respectively. These levels are quite small relative to the total density difference (Fig. 3).

The relative temperature of tributary and reservoir surface waters varied seasonally, with WBDR and TC being warmer in spring and cooler from mid-summer through fall (Owens 1998a), resulting in a seasonal density difference (Fig. 3). Variations in conductivity also existed between tributaries and the reservoir surface (Fig. 4), but again the contribution of conductivity to variations in density is negligible. This allows conductivity (or *TDS*) to be used as a passive (not affecting water motion through buoyancy effects) tracer in the reservoir.

Variations in the relative density of tributary and

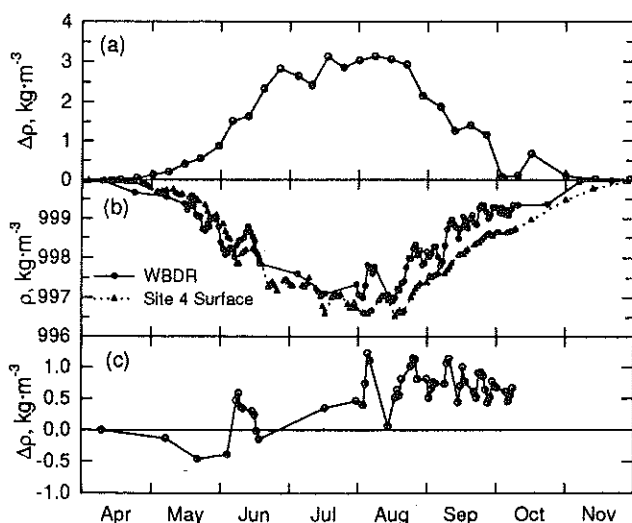


Figure 3.—Density of reservoir and tributary waters: (a) difference in density between bottom and surface waters of reservoir at site 1; (b) density of reservoir surface at site 4, and of WBDR; and (c) difference in density between WBDR and site 4 surface on days that temperature measurements of both waters were made.

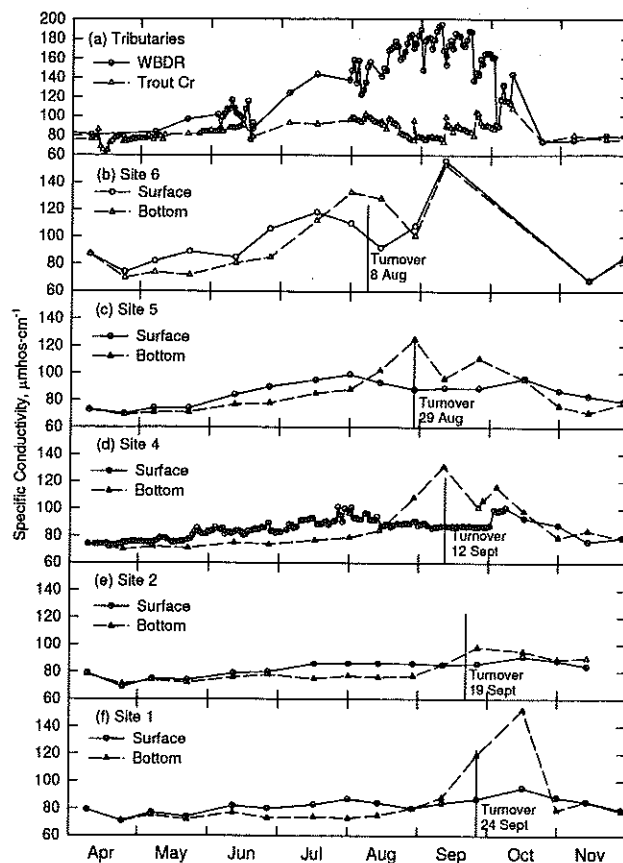


Figure 4.—Variation of conductivity during 1995: (a) West Branch Delaware River and Trout Creek; (b) surface and bottom at site 6; (c) surface and bottom at site 5; (d) surface and bottom at site 4; (e) surface and bottom at site 2; (f) surface and bottom at site 1. The plots from reservoir sites also indicate the observed occurrence of fall turnover (vertical homogeneity in temperature) at each site.

reservoir surface waters indicate that a seasonal shift in the inflow mixing regime occurs in the reservoir. When the tributary is less dense than reservoir surface waters, a buoyant overflow occurs, so that tributary inflow is mixed directly into the upper mixed layer of the reservoir (Ford and Johnson 1983, Alavian et al. 1992). When the tributary is more dense, a plunging density current forms, where the negatively-buoyant tributary waters flow down the submerged river channel as a relatively distinct current, until its density is equal to that of the reservoir water column at a particular depth, at which point an interflow occurs and the tributary inflow effectively enters the reservoir water column (Ford and Johnson 1983, Alavian et al. 1992). The vertical position of the effective entry, or "neutral buoyancy," may be estimated by locating the elevation in the reservoir water column where the temperature is equal to that of the inflow. During 1995, an overflow occurred from spring until early June, after which the position of neutral buoyancy was at or slightly above the thermocline until fall turnover in October (Fig. 2).

A potential impact of plunging or negatively-buoyant tributary inflows on reservoir water quality is the formation of metalimnetic oxygen minima. This condition is defined as the existence of low concentration of dissolved oxygen (DO) in the area of the metalimnion relative to the epilimnion above or the hypolimnion below (Wetzel 1983). In a detailed analysis of observations from DeGray Lake that included metalimnetic oxygen minima, Nix (1981) found that the neutral buoyancy depth for the major reservoir inflow was at the same vertical position as the lowest metalimnetic DO concentration over the period of time that the minimum existed. Together with other evidence, Nix (1981) concluded that the minima was caused by the transport of oxygen-demanding materials from upstream into the metalimnion by the plunging tributary inflow. A similar analysis of 1995 Cannonsville Reservoir data indicates that the neutral buoyancy depth for the WBDR inflow is consistently 3 to 6 m higher in the water column than the point of minimum metalimnetic DO concentration (Fig. 5), indicating that the source for the oxygen-demanding materials is not the tributary inflow. An alternative source of organic material may be settling from the productive epilimnion (Nix 1981, Wetzel 1983).

The conductivity of TC was relatively constant over the 1995 monitoring period, while WBDR conductivity increased from May through mid-September, and decreased rapidly thereafter (Fig. 4a). Conductivity in the reservoir apparently responded to these variations in the major inflow, with gradual increases over the summer (Fig. 4). At all reservoir monitoring sites, the bottom conductivity was less than the surface conductivity from spring to mid-summer, with a sudden increase in bottom conductivity to levels higher than surface occurring in late summer (Fig. 4). The only possible source of water of such elevated conductivity is WBDR, and its appearance at the bottom of the water column at various reservoir sites is an indication that WBDR is negatively buoyant and is plunging to the bottom once thermal stratification is lost at a particular site. There is a lag in time at which elevated conductivity is detected in the bottom waters (Fig. 4b through 4f), indicating that the WBDR inflow does not plunge to the bottom until the thermal stratification has weakened at a particular site.

### *Estimation of longitudinal dispersion coefficient*

The observed dynamics of inflow conductivity (Fig. 4a) and the observed longitudinal gradient in conductivity in the epilimnion of the reservoir (Fig. 4b through 4f) presents the opportunity to estimate the

longitudinal dispersion coefficient in the epilimnion through the application of a mass transport model. While a detailed two-dimensional (vertical and longitudinal) numerical mass transport model has been developed for the reservoir (Gelda et al. 1998), a simple analytical model is used here to provide an estimate of the average dispersion coefficient over the period May-August 1995. This estimate is based on the following assumptions: (1) the epilimnion of the WBDR arm and main basin of the reservoir is assumed to be a "channel" of constant cross-sectional area from the mouth of the WBDR to the dam; (2) mass transport at the base of this assumed channel, or between the epilimnion and hypolimnion, is neglected; (3) only flow from WBDR is considered, and this flow enters the channel at the upstream end and exits at the downstream end; (4) the waterflow, resulting flow velocity, and dispersion coefficient are constant.

Under these conditions, the analytical solution for an instantaneous source of mass  $M$  at the upstream end of the reservoir is (Thomas and McKee 1944)

$$C = 2 \frac{M}{V} \sum_{i=1}^{\infty} \frac{a_i L \exp(-k_i^2 \frac{t}{L} + \frac{Pe}{2} \frac{x}{L})}{a_i^2 L^2 + Pe^2/4 + Pe} [a_i L \cos(a_i x) + \frac{Pe}{2} \sin(a_i x)] \quad (1)$$

where  $C$  is concentration,  $V$  and  $L$  are the volume and length of the channel representing the epilimnion,  $x$  is the longitudinal position ( $x=0$  at upstream end),  $t$  is time,  $t=L/U$  is the detention time in the epilimnion,  $Pe=UL/E$  is the Peclet number,  $U$  is the flow velocity through the epilimnion,  $E$  is the longitudinal dispersion coefficient, and  $a_i$  are the roots of the implicit equation given by

$$\cot(a_i L) = \frac{a_i L}{Pe} + \frac{Pe}{4a_i L}$$

and

$$k_i^2 = \frac{a_i^2 L^2}{Pe} + \frac{Pe}{4}$$

This simple analytical model was applied to the epilimnion of Cannonsville Reservoir for the 4-month period from 1 May, when increases in WBDR conductivity began (Fig. 4a), until 31 August, when deepening of the thermocline and plunging of the WBDR inflow were occurring. During this period, longitudinal conductivity gradients were observed in the epilimnion (Fig. 4). The assumed geometric properties of the rectangular channel representing the epilimnion were  $L=22.5$  km, and depth and width equal to 7 and 400 m, respectively. The average WBDR flow rate for this period of  $3.6 \text{ m}^3 \cdot \text{s}^{-1}$  resulted in a velocity  $U=0.13 \text{ cm} \cdot \text{s}^{-1}$ .

As Eq. 1 is a solution to the linear advection-

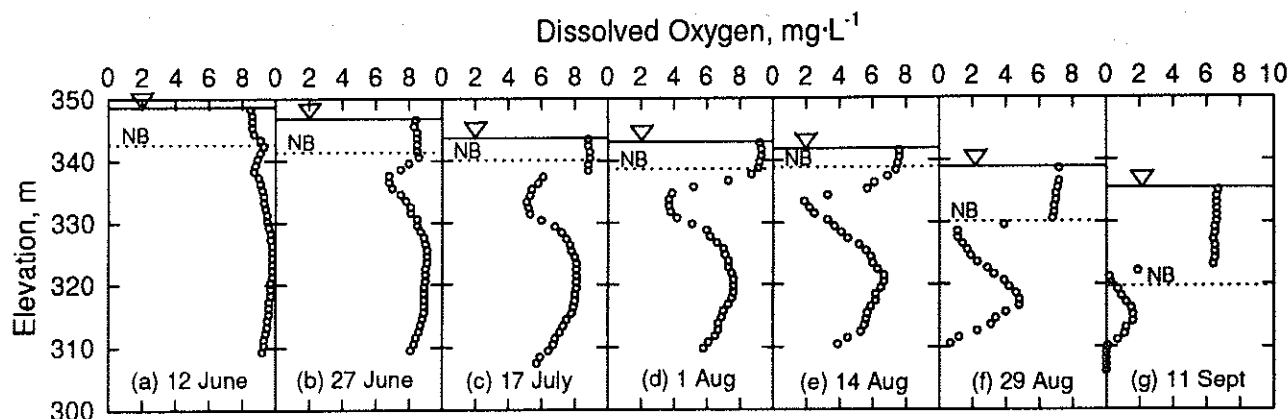


Figure 5.—Dissolved oxygen profiles during period of metalimnetic oxygen minima in 1995: (a) 12 June; (b) 27 June; (c) 17 July; (d) 1 August; (e) 14 August; (f) 29 August; and (g) 11 September. Also shown is the elevation of neutral buoyancy (NB) at which temperature of West Branch Delaware River matches the water column temperature at site 4.

dispersion equation for an instantaneous source, the solution for a continuous source can be computed by superposition of a series of instantaneous sources of varying magnitude over time. Also, as the advection-dispersion equation represents a mass conservation principle, observations of conductivity were converted to *TDS* for use in Eq. 1. The observed time variation of inflow conductivity (Fig. 4a) was used to define a time series of equivalent daily mass loadings of *TDS* which was introduced at the upstream end of the channel. The use of Eq. 1 also assumes that *TDS* is conservative in the reservoir. The only unknown in this analysis is then the dispersion coefficient *E*. The estimated value of  $E = 13 \text{ m}^2 \cdot \text{s}^{-1}$  was determined by minimizing the difference between computed and observed concentrations of *TDS*. Given the nature of the assumptions necessary to apply this simple analytical model, the agreement between computed and observed concentrations (Fig. 6) is reasonably good.

### Analysis of vertical transport

As vertical gradients in conductivity were weak and not well-defined when compared to longitudinal gradients, temperature is the only tracer that may be used to evaluate vertical mixing. To evaluate the relative magnitudes of advection and diffusion on vertical transport, a heat budget was calculated for the portion of the reservoir volume below elevation 335.0 m (Fig. 7a) for the period 1 June through 15 August 1995. This elevation was selected because it is 2 m above the top of the withdrawal structure used during this period, so that it can be assumed that all outflow occurred from the water column below this elevation. In addition, during this time the thermocline was located above this elevation, so that all inflow

(including the effects of plunging inflow) entered the water column above this elevation. As a result, a water balance on this constant volume states that the outflow (dam release  $Q_R$  plus drinking water withdrawal  $Q_D$ ) is equal to the inflow (Fig. 7a). This inflow is idealized as a vertical waterflow across the area at the top of the volume. The total rate of heating of this water volume  $\Phi_T$  is given by

$$\Phi_T = \rho c V_L \frac{dT_L}{dt} \quad (2)$$

where  $c$  is the specific heat of water, and  $V_L$  and  $T_L$  are the volume and average temperature of the layer. It is assumed that the total rate of heating has components due to advection (vertical water motion) and diffusion. The advection component is computed by

$$\Phi_A = \rho c [(Q_R + Q_D) T_{335} - Q_R T_R - Q_D T_D] \quad (3)$$

where  $T_{335}$ ,  $T_R$  and  $T_D$  are temperatures in the water column at elevation 335, of the dam release and of drinking water withdrawal, respectively.

Determination of the temperatures in Eqs. 2 and 3 indicates that inflow into the layer is warmer than the layer itself ( $T_{335} > T_L$ ), while the dam release flow is cooler (Fig. 7b), leading to the result that  $\Phi_A$  is a positive quantity (Fig. 7c). Comparison of the relative magnitudes of  $\Phi_T$  and  $\Phi_A$  indicates that vertical advection dominates the process of heating of the lower waters of the reservoir over this period (Fig. 7d).

### Temperature of Outflows

The temperature of water leaving the reservoir through the active drinking water intake generally increases over the period of thermal stratification in

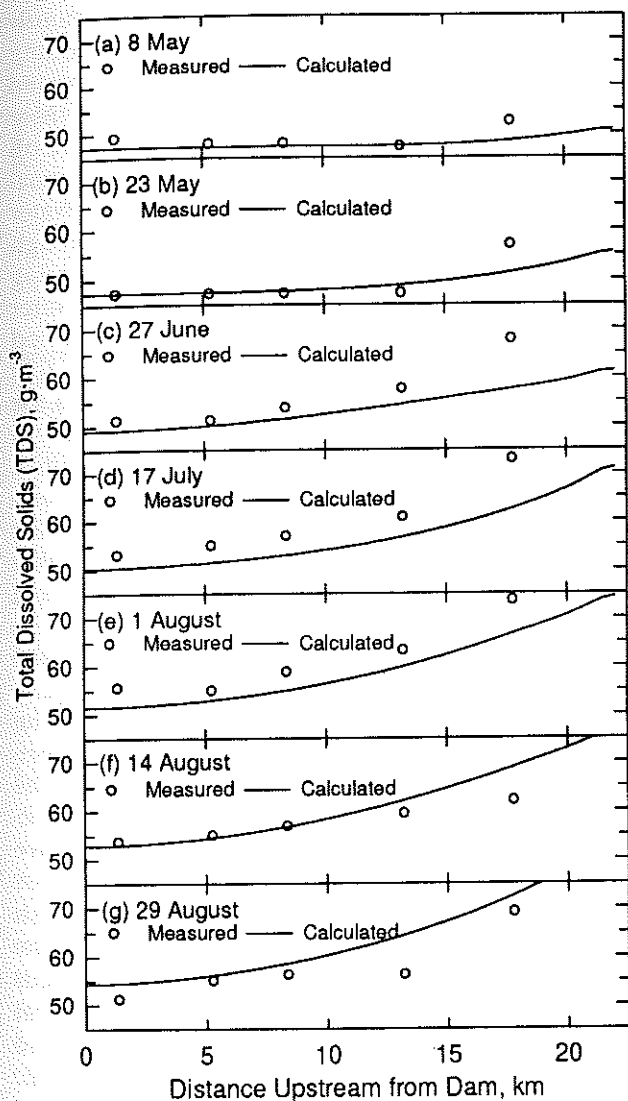


Figure 6.—Variation of total dissolved solids concentration with longitudinal position on various dates during the summer of 1995: (a) 8 May; (b) 23 May; (c) 27 June; (d) 17 July; (e) 1 August; (f) 14 August; and (g) 29 August. Observations (computed from measured conductivity) and predictions of analytical model using dispersion coefficient  $E=13 \text{ m}^2 \cdot \text{s}^{-1}$  are shown.

the reservoir (Fig. 8a). During 1995, the middle intake was used until late August, when significant drawdown forced the use of the lower intake until mid-September, when withdrawal was discontinued until late November. During periods when thermal stratification is present in the reservoir, matching of the withdrawal temperature to that occurring at a certain vertical position in the water column can be used to indicate the position from which the intake is effectively drawing water. The apparent withdrawal elevation so determined corresponds well to the vertical position of the intake opening (Fig. 8b).

Similarly, the water temperature observed in the

river channel downstream of the dam also increased through the summer stratification period (Fig. 8a). Matching of dam release temperature with a water column temperature at site 1 determined the apparent vertical position in the water column from which dam release draws water. The resulting elevations were much higher than the actual elevation of the release point and varied over time. Similar results were obtained in the analysis of observations from previous years.

### Thermistor Chain Measurements

The thermistor chain at site 1 observed the approach to fall turnover, and subsequent cooling of the water column during the turnover period (Fig. 9a).

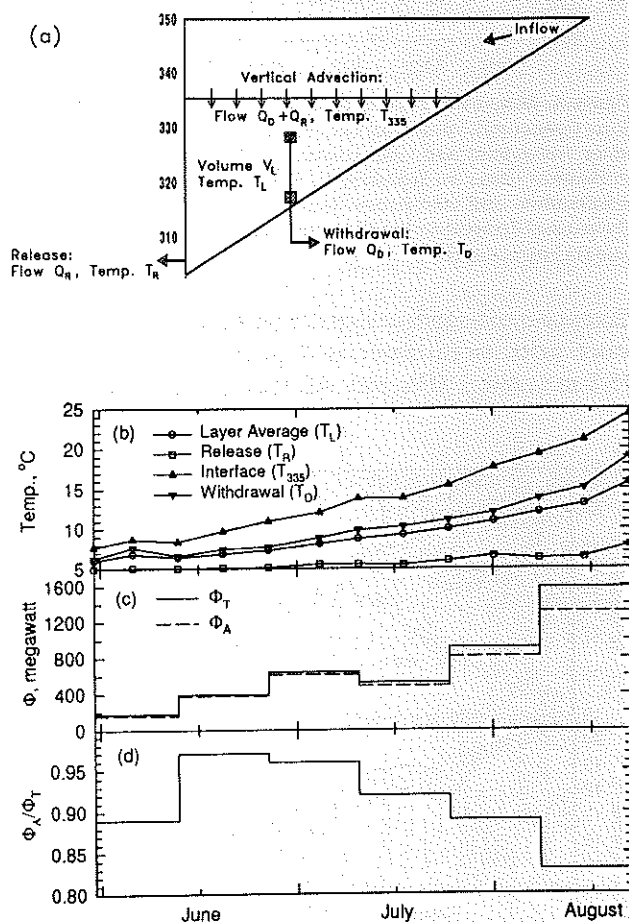


Figure 7.—Estimation of the contribution of advection to the vertical transport of heat to the lower waters of the reservoir for the period 1 June through 15 August: (a) schematic of heat balance computed on water volume in reservoir below elevation 335 ( $V_L$ ), including average temperature of the layer  $T_L$ , flow  $Q_R$  and temperature  $T_R$  of dam release, and flow  $Q_D$  and temperature  $T_D$  of drinking water withdrawal; (b) variation of average reservoir temperature below elevation 335 ( $T_L$ ), temperatures of dam release ( $T_R$ ) and withdrawal ( $T_D$ ), and temperature at elevation 335 ( $T_{335}$ ); (c) total rate of heating  $\Phi_T$  and rate of heating associated with vertical advection ( $\Phi_A$ ); and (d) ratio  $\Phi_A/\Phi_T$ .



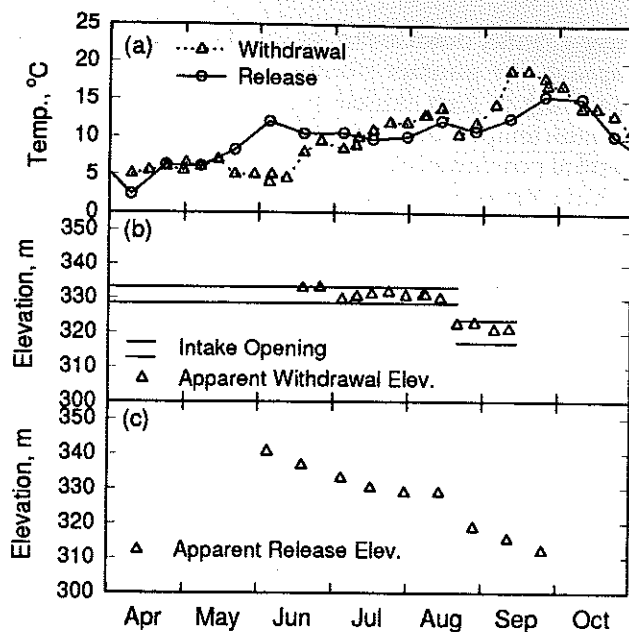


Figure 8.—Measurements and analysis of temperature of outflows from Cannonsville Reservoir for 1995: (a) temperature of drinking water withdrawal and dam release; (b) effective elevation of withdrawal based on matching of withdrawal and water column temperature, and elevation of intake openings; and (c) effective elevation of dam release based on matching of dam release and water column temperatures.

Transport of heat downward causes increasing temperature prior to turnover at depths of 13.8, 16.3, and 18.8 m at site 1 (Fig. 9a). At depths less than 13.8 m,

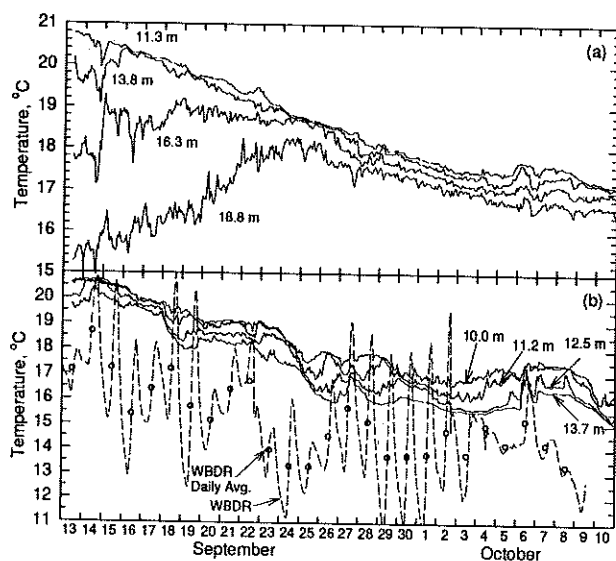


Figure 9.—Selected measurements from thermistor chains in Cannonsville Reservoir, September and October 1995: (a) observed temperatures at site 1 at depths of 11.3, 13.8, 16.3, and 18.8 m; (b) observed temperatures at site 4 and of West Branch Delaware River inflow. With the exception of diurnal stratification near the surface, vertical variation in temperature was less than 2 °C above the shallowest depth shown.

temperatures were uniform and were continuously falling during the period of deployment, indicating thermistors at depths less than 13.8 m were located in the deepening epilimnion. The lowest thermistor (18.8 m depth) reaches a maximum temperature on 25 September. It is interesting to note that thermal stratification was present near the bottom of the water column over the period from 25 September through 10 October, even though temperatures were decreasing at all depths on the chain. The more shallow water column at site 4 was largely unstratified for the period of thermistor chain deployment (Fig. 9b), in that temperatures at all depths were decreasing. As in the case of thermistor observations after 25 September at site 1, weak thermal stratification was present at site 4 throughout the deployment period (Fig. 9b). A comparison of the thermistor measurements at site 4 to the WBDR temperatures for the same period indicates that the relatively cold inflow may act as a source of cold water at the bottom of the water column (Fig. 9b).

The thermistor observations at both sites 1 and 4 indicate higher frequency fluctuations in temperature. For thermistors that are located in the deepening epilimnion, these fluctuations are affected by short-term variations in meteorological conditions. In the stratified hypolimnion at site 1 (Fig. 9a), these fluctuations are likely to be associated with internal wave (internal seiche) activity. As spectral analysis of the time series of temperature observations at the 18.8 m depth over the period from 13 to 24 September indicates the presence of several characteristic or dominant periods of oscillation (Fig. 10). Roschek (1996) has found that these frequencies are in close agreement with those predicted by a simple two-layer model of frictionless, unforced internal wave oscillations.

### Observations of Currents

Currents observed at sites 1 and 4 were episodic, with events of significant speeds ( $>2 \text{ cm} \cdot \text{s}^{-1}$ ) separated by periods with no (or undetectably low) currents lasting for several days or more (Fig. 11c and 11d). The location of the current meters during the early fall deployment period was such that no significant thermal stratification was present above the level of the meters at either site, so that the effect of wind stress (Fig. 11a) would not be dampened at depth by the presence of the thermocline. Wind events occurred on 13 September, 26 September, and 4 to 5 October (Fig. 11a), with coincident events in current speed (Fig. 11c and 11d). It might also be expected that reservoir outflow would affect currents, particularly at nearby sites. For example, dam release was in the range of  $15$  to  $30 \text{ m}^3 \cdot \text{s}^{-1}$  for most of this period, but was

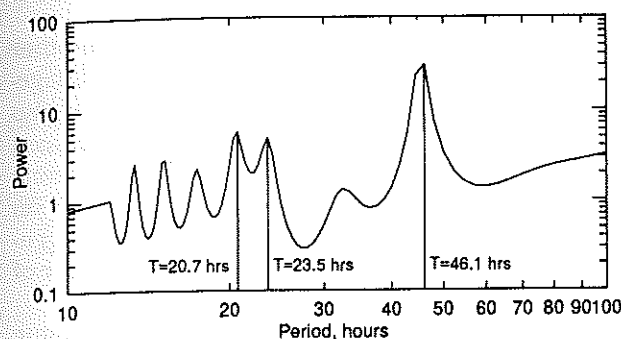


Figure 10.—Spectral analysis of temperature time series measured by thermistor string deployed at site 1 at 18.8 m depth, from 13 to 24 September 1995.

abruptly reduced to nearly zero on 4 October (Fig. 11b), which may in part explain currents occurring at nearby site 1 (Fig. 11c). Drinking water withdrawal ceased on 14 September for the remainder of the deployment period, while reservoir inflow was generally low for the entire period (Fig. 11b).

## Discussion

Several of the observations described above support the conclusion that, during late summer and fall, the inflow from WBDR formed a negatively-buoyant density current. Comparison of WBDR and water column temperatures from the deepest monitoring site indicates that the neutral buoyancy (equal temperature) depth generally follows the thermocline as it drops in elevation over this period. As the thermocline drops, thermal stratification is progressively lost from shallow (8 August at site 6; Fig. 4b) to deep locations (24 September at site 1; Fig. 4f). After turnover has occurred at a particular site, it would be expected that the presence of the plunging inflow would be detected at the bottom of the water column. This was found in observations of conductivity at sites 6, 5, 4, 2, and 1 (Figs. 4b through 4f) and temperature at sites 4 and 1 (Fig. 9). Prior to turnover at a particular site, elevated conductivity at the thermocline was occasionally detected in vertical profiles (not shown), indicating the presence of interflow from WBDR.

In a lake or reservoir where temperature dynamics are driven solely by heat and momentum transfer at the water surface, temperature variations in the days prior to fall turnover would typically involve decreasing temperatures in the epilimnion in response to loss of heat at the water surface, together with increasing temperature in the hypolimnion resulting from transport of heat from the epilimnion into the hypolimnion. These processes continue until the tem-

peratures of the warming hypolimnion and the cooling epilimnion meet, at which time fall turnover begins. Following the onset of turnover, the continued loss of heat at the water surface together with wind-driven mixing and buoyancy-driven convection causes the entire water column to be isothermal during this cooling period, until the temperature of maximum density at 4 °C is reached.

The thermistor chain observations at site 1 (Fig. 9a) are consistent with this progression until 24 September, when the temperature at 18.8 m reaches a maximum. Thereafter, the bottom waters at site 1 are cooling at the same time that weak thermal stratification persists in the water column. Thus, there must be a source of cold water which causes the bottom waters to remain cooler than the surface; the only possible source is the tributaries (Fig. 9b). Temperature analysis of WBDR and TC indicates that TC is consistently cooler than WBDR in summer and fall (Owens 1998a), and thus will also tend to plunge. However, the much lower flow of TC (Owens et al. 1998) indicates that the effect of plunging may be difficult to detect in the reservoir.

Reservoir intake structures typically draw water from the reservoir over a range of depth extending above and below the level of the structure itself. The range of depth, and the distribution of flow from that range, depend on the geometry of the inflow structure, local reservoir bathymetry, and thermal stratification

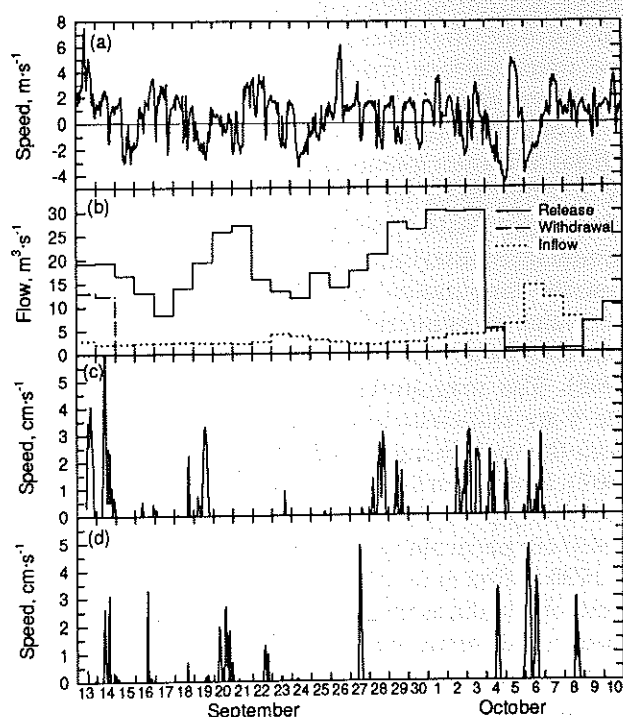


Figure 11.—Observed time series of: (a) wind speed at Cannonsville Dam meteorological station; (b) total reservoir inflow, dam release, and drinking water withdrawal; (c) current speed at site 1, elevation 323.0 m; and (d) current speed at site 4, elevation 323.6 m.



in the vicinity of the intake elevation (Davis 1987). The analysis of temperature of drinking water withdrawal indicates that this range of depth is not significantly skewed in the vertical elevation so that, while the intakes may draw water from above and below the elevation of the intake itself, the resulting mix of water closely resembles, at least in temperature, water at the level of the intake. However, the temperature of dam release is significantly higher than that found near the bottom of the dam at the elevation of the release tunnels. While it is possible that the elevation of the thermocline may be reduced in the immediate vicinity of the release point, it is more likely that significant heating of the water released occurs over the 2.4-km channel between the base of the dam and the temperature monitoring station downstream of the dam.

Vertical transport in a reservoir may be decomposed into advection and diffusion processes (Fischer et al. 1979). Advection describes the net downward water motion associated with shoreline inflows and deep withdrawal or release. Diffusion refers to the turbulent mixing that is driven by wind shear at the water surface and is damped by thermal stratification (Fischer et al. 1979). The fact that the observed rate of heating of the lower waters of the reservoir can be largely explained by advection (Fig. 7) indicates that diffusion played a relatively small role during the stratification period of 1995. This may be explained by the unusually large drawdown during 1995 (Fig. 2), or by the steep hillsides that surround the reservoir basin, which partially shelter the water surface from wind shear and resulting turbulent mixing.

Longitudinal gradients in temperature (Owens 1998a) and water quality (Effler and Bader 1998) have been found to be modest in Cannonsville Reservoir. The longitudinal dispersion coefficient, estimated from conductivity observations, may be used in models that describe longitudinal variation (Gelda et al. 1998). The value so estimated ( $E=13 \text{ m}^2 \cdot \text{s}^{-1}$ ) is in the range found for other reservoirs (Fischer et al. 1979, Martin 1988). The magnitude of the observed currents at site 4 are sufficient to cause sediment resuspension from the underlying bottom (Lemmin and Imboden 1987). It has been found that resuspension of particles containing phosphorus is significant in Cannonsville Reservoir, particularly in the late summer and early fall of 1995 (Effler et al. 1998). It may be concluded from these observations that resuspension from the pelagic (deep) sediments may contribute to the total resuspension.

In summary, transport processes that affect the vertical and longitudinal distribution of heat and mass constituents in Cannonsville Reservoir have been identified and, in some cases, quantified. The plunging inflow phenomenon may affect the vertical and

longitudinal distribution of nutrients, DO and other constituents, and thus should be included in management models of the reservoir. These models may also be used to further investigate the relationship between plunging inflow and metalimnetic oxygen minima (Fig. 5). Water quality modeling of this condition would allow comparison of the quantity of oxygen-demanding materials in the inflow to the magnitude of DO depletion observed in the metalimnion.

The data described here may be used to calibrate and confirm hydrothermal models of the reservoir. Model reproduction of the observed rate of hypolimnetic heating, particularly over multiple years that encompass varying levels of release and drawdown, would indicate accurate simulation of vertical transport. A two-dimensional model (Gelda et al. 1998) may be used to reproduce the longitudinal gradient in conductivity and the observed short-term variations in temperature and water motion. Accurate hydrothermal model hindcasting of these observations would indicate that the models may be applied with confidence in the investigation of water quality management alternatives.

**ACKNOWLEDGMENTS:** Support for this study was provided by the New York City Department of Environmental Protection. C. J. Roschek aided in the deployment of the thermistor strings and in data analysis.

## References

- Alavian, V., G. H. Jirka, R. A. Denton, M. C. Johnson and H. G. Stefan. 1992. Density currents entering lakes and reservoirs. *J. Hydr. Engr.* 118(11):1464-1489.
- Chapra, S. C. 1997. *Surface water-quality modeling*. McGraw-Hill Book Co.
- Davis, J. E. 1987. SELECT: A numerical one-dimensional model for selective withdrawal. Instruction Rep. E-87-2, U.S. Army Engineer Waterways Experiment Sta., Vicksburg, MS.
- Effler, S. W. and A. P. Bader. 1998. A limnological analysis of Cannonsville Reservoir, NY. *Lake and Reserv. Manage.* 14(2-3):125-139.
- Effler, S. W., R. K. Gelda, D. L. Johnson and E. M. Owens. 1998. Sediment resuspension in Cannonsville Reservoir. *Lake and Reserv. Manage.* 14(2-3):225-237.
- Fischer, H. B., E. J. List, J. Imberger, R. C. Y. Koh and N. G. Brooks. 1979. *Mixing in Inland and Coastal Waters*. Academic Press.
- Ford, D. E. and M. C. Johnson. 1983. An assessment of reservoir density currents and inflow processes. Tech. Rep. E-83-7, Environ. Lab. U.S. Army Waterways Experiment Station, Vicksburg, MS.
- Gelda, R. K., E. M. Owens and S. W. Effler. 1998. Calibration, verification, and an application of a two-dimensional hydrothermal model for Cannonsville Reservoir. *Lake and Reserv. Manage.* 14(2-3):186-196.
- Lemmin, U. 1987. The structure and dynamics of internal waves in Baldegersee. *Limnol. Oceanogr.* 32(1):43-61.
- Lemmin, U., and D. M. Imboden. 1987. Dynamics of bottom currents in a small lake. *Limnol. Oceanogr.* 32(1):62-75.
- Martin, J. L. 1988. Application of two-dimensional water quality model. *J. Environ. Engr.* 114(2):317-336.

- Nix, J., 1981. Contribution of hypolimnetic water on metalimnetic dissolved oxygen minima in a reservoir. *Water Resources Res.* 17(2):329-332.
- Owens, E. M. 1998a. Thermal and heat transfer characteristics of Cannonsville Reservoir. *Lake and Reserv. Manage.* 14(2-3):152-161.
- Owens, E. M. 1998b. Development and testing of one-dimensional hydrothermal models of Cannonsville Reservoir. *Lake and Reserv. Manage.* 14(2-3):172-185.
- Owens, E. M., R. K. Gelda, S. W. Effler and J. M. Hassett. 1998. Hydrologic analysis and model development for Cannonsville Reservoir. *Lake and Reserv. Manage.* 14(2-3):140-151.
- Roschek, C. J. 1996. Field monitoring and modeling of the internal seiche in Cannonsville Reservoir. M.S. Thesis, Dept. of Civil and Environmental Engr., Syracuse Univ., Syracuse, NY.
- Thomas, H. A. and J. E. McKee. 1944. Longitudinal mixing in aeration tanks. *Sewage Works Journal.* 16(1):42-55.
- Wetzel, R. G. 1983. *Limnology*. Saunders College Publishing.